University of Baghdad
College of Engineering
JOURNAL OF ENGINEERING

**Journal of Engineering**
journal homepage: www.joe.uobaghdad.edu.iq
Number 7 Volume 25 July 2019

***Mechanical and Energy Engineering***

# Numerical Study of Fluid Flow and Heat Transfer Characteristics in Solid and Perforated Finned Heat Sinks Utilizing a Piezoelectric Fan

**Ayser Shamil Salman**
Mechanical Engineering Department
College of Engineering- Baghdad University
E-mail: aysser.alhassan@gmail.com

**Asst. Prof. Dr. Mohammed A. Nima***
Mechanical Engineering Department
College of Engineering- Baghdad University
E-mail: dralsafi@uobaghdad.edu.iq

## ABSTRACT

Numerical study is adapted to combine between piezoelectric fan as a turbulent air flow generator and perforated finned heat sinks. A single piezoelectric fan with different tip amplitudes placed eccentrically at the duct entrance. The problem of solid and perforated finned heat sinks is solved and analyzed numerically by using Ansys 17.2 fluent, and solving three dimensional energy and Navier–Stokes equations that set with RNG based k−ε scalable wall function turbulent model. Finite volume algorithm is used to solve both phases of solid and fluid. Calculations are done for three values of piezoelectric fan amplitudes 25 mm, 30 mm, and 40 mm, respectively. Results of this numerical study are compared with previous both numerical and experimental studies and give a good agreement. Numerical solution is invoked to explain the behavior of air flow and temperature distribution for two types of circular axial and lateral perforations. For each type, all the results are compared with an identical solid finned heat sink. Perforations show a remarkable enhanced in the heat transfer characteristics. The results achieved enhancement in the heat transfer coefficient about 12% in axial perforation and 25% in the lateral perforation at the maximum fan amplitude.

**Key words:** piezoelectric fan, heat transfer, axial perforated heat sink, laterals perforated heat sink.

# دراسة عددية لخصائص جريان المائع وانتقال الحرارة في مصب حراري صلب ومثقب مجهز بمروحة كهروضغطية

**أيسر شامل سلمان**
قسم الهندسة الميكانيكية
كلية الهندسة – جامعة بغداد

**أ.م.د. محمد عبد الرؤوف نعمة**
قسم الهندسة الميكانيكية
كلية الهندسة – جامعة بغداد

## الخلاصة

قدمت هذه الدراسة العددية فكرة للجمع بين مروحة كهرضغطية كمولّد لتدفق هواء مضطرب ومصبات حرارية مزعنفة ذات ثقوب طولية وعرضية. وتم تشغيل مروحة كهرضغطية واحدة بسعات مختلفة وثبتت بشكل مركزي في مدخل مجرى الهواء. تم حل ودراسة تاثير الجريان الناتج عن المروحة على المصبات الحرارية المزعنفة الصلبة والمثقبة وتحليلها عدديًا باستخدام برنامج (Ansys 17.2، فلونت) وحل معادلات ثلاثية الأبعاد ومعادلات Navier – Stokes التي تم ضبطها مع نموذج مضطرب قابل للتطوير يعمل على أساس RNG k−ε باستخدام طريقة

*Corresponding author
Peer review under the responsibility of University of Baghdad.
https://doi.org/10.31026/j.eng.2019.07.05

Article received: 27/3/2018
Article accepted: 28/6/2018

(Finite volume) لحل تاثر انتقال الحرارة بجريان المائع. تم حساب ثلاث معدلات لدرجة الحرارة الناتجة من تغيير سعة المروحة الكهرضغطية (25 مم و 30 ملم و 40 ملم) على التوالي. تم مقارنة النتائج المستحصلة من هذه الدراسة العددية بالدراسات العددية والتجريبية السابقة ووجدت موافقة جيدة. تم اجراء الحل العددي لشرح سلوك تدفق الهواء وتوزيع الحرارة لنوعين من الثقوب المحورية والجانبية الدائرية. لكل نوع ، تم مقارنة جميع النتائج الخاصة بالمصبات المثقبة مع مصب بزعانف صلبة ومتطابقة بالابعاد والظروف فظهر تحسناً ملحوظاً في خصائص انتقال الحرارة بنسبة 12% في التثقيب الطولي و 25% في التثقيب المستعرض عند السرعة الاعلى للمروحة.
**الكلمات الرئيسية:** مروحة كهروضغطية، انتقال حرارة، مصب حراري مثقب طوليا، مصب حراري مثقب عرضيا.

## 1. INTRODUTION

The aim of many studies and researches are improving the performance of the fins to the highest levels and reduce both the cost of production and the weight, especially in the electronic and microelectronic devices. To achieve these goals, one of these ways is making surface perforations. This study is an attempt to twinning the work of finned heat sinks with a piezoelectric fan, trying to predict the effects of changing the speed of the fan tips and the effect of both increasing the number of perforations and its diameter. The piezoelectric fan is relatively modern cooling equipment used with electronic devices due to its noiseless, light weight, and long life.

Comprehensive study deduced by **Sara, 2001** studied experimentally the enhancement of heat transfer from a flat surface in a rectangular channel flow by attached perforated rectangular cross sectional blocks as function of the flow and geometrical parameters. They mentioned that perforations in the blocks enhance heat transfer and the enhancement increases with increasing the perforation inclination angle and degree of perforations. **Torii,** and **Yang, 2002** studied theoretically an unsteady, 2-dimensional, incompressible thermal-fluid flow over both sides of a slot-perforated flat surface, which is placed in a pulsating free stream. And found that an amplification of heat-transfer performance when the free stream is pulsated, and the heat-transfer performance at the rear plate is induced with an increase in both Reynolds number and perforation diameter to plate thickness ratio. **Açıkalın, et al., 2003,** studied numerically the influence of two dimensional steady state incompressible flows induced by tinkling blades. They foretell analyze solutions that offered for an infinite beam. Also they avail the results as boundary conditions to predict the behavior of flows generated by a vibrated piezoelectric fan. Therefore, they found compatibility with the experimental flows behavior. **Açıkalın, et al., 2004,** studied experimentally the benefit and limitation of inserting fans in a real electronic device, and observed highly increase in heat transfer and concluded these types can't replace the rotary fans. **Dorignac, et al., 2005,** studied experimentally convective heat transfer from multi perforated plate. For an extensive of perforations spacing, they drive an empirical relation for heat exchange at the windward surface of a perforated flat plate. Results shown the independence of heat transfer coefficients and effectiveness from the jet injection temperature within the range studied. The influence of confinement on heat transfer coefficient is weak, but it has a great impact on effectiveness. **Kimber, et al., 2007,** analyzed experimentally both single and multi-piezoelectric fans, studied different both fan amplitudes and distance relative to the heated stainless steel sheets. By using an infrared camera they found the optimal distance relative to the hot sheets varied according to the piezoelectric fan amplitude. **Sahin,** and **Demir, 2008,** investigated experimentally the

variation of overall heat transfer, friction factor and effect of different design parameters on heat transfer and friction factor for heat exchangers prefabricated with square cross sectional perforated pin fins in a rectangular channel. They considered the effect of flow and geometrical parameters on heat transfer and friction characteristics and gained correlations for the efficiency enhancement. **Shaeri,** and **Yaghoubi, 2009,** worked numerically on a three-dimensional array of rectangular perforated fins with square holes that were arranged in a lateral side and longitudinal fins. The Navier–Strokes equations and RNG based k–$\varepsilon$ turbulent model were utilized. Fin efficiency in perforated form was determined and compared with the equivalent solid fin. They found that new perforated fins have higher total heat transfer and considerable weight reduction as compared with solid fins. **Petroski, et al., 2010,** experimentally placed a fan on the fin side of the base of a heat sink and conducted flow visualization tests to validate flow models developed using commercially available CFD software. Heat transfer measurements were also done to measure the increase in cooling performance. This represents the first known attempt to merge a fan of this structure into a heat rejection device. **Wadhah, 2011,** investigated experimentally enhancement of natural convection heat transfer from rectangular fins by circular perforations. He found that the heat transfer rate and the coefficient of heat transfer increases with an increased perforations number. **AIEssa, et al., 2012,** examined experimentally the heat dissipation from a horizontal rectangular fin with square perforation, and rectangular perforations with an aspect ratio of two, equilateral triangular perforations of bases parallel and towards its fin tip utilizing the finite element technique under natural convection. He compared the results between the perforated fin and its external dimensionally equivalent solid fins. He found that perforations in the fins enhance heat dissipation rates.

To the limit of researchers' knowledge, there is no existent study running the same field which collecting both a piezoelectric fan and perforated finned heat sinks. So this numerical study addresses to forecast the behavior of both turbulent air flow and heat dissipation with convection effects. In the scope of work, a piezoelectric fan has a three different tip speed (25mm, 30 mm, and 40 mm) used to generate air flow which is exposed to a ducted both axial and lateral perforated finned heat sinks which they existing to constant heat flux 4340 W/m$^2$. So this study is trying to explain the effects of the piezoelectric fan on heat transfer characteristics and calculate the amount of the enhancing in the heat transfer coefficient and the effectiveness with different porosities and compared to identical solid finned heat sink results.

## 2. ABRIEF DESCRIPTION OF PROBLEM AND ITS BOUNDARY CONDITIONS

Typically the presentation of finned heat sink with the piezoelectric fan was modeled in this study as shown in **Fig. 1**. The base is considered to be from Teflon with dimensions length, width, and height (200 mm, 120 mm, and 30 mm) respectively, the heater is the only heat source with constant heat flux, its dimensions length, width, and height are (50 mm, 50 mm, and 0.8 mm) respectively the heat sink supposed to be from aluminum alloys with thermal conductivity 202 Wm$^{-1}$ K$^{-1}$. The base length, width, and height dimensions (50 mm, 50 mm, and 3 mm) respectively with four fins each fin is length, width, and height dimensions (50 mm, 4 mm, and 30 mm). The number of studied heat sinks are ten, one of them is solid and the others are divided in to two groups the axial perforated group with constant perforation diameter and increasing the number of

perforations and the lateral perforated group, also the lateral group is divided to two subgroups as shown in **Fig. 1**, the constant perforation diameter with increasing the number of perforations and the constant number of perforation with increasing the perforations diameter. The heat sink and the piezoelectric blade covered with a three mm thickness Perspex duct with dimensions in length, width, and height (135 mm, 70 mm, and 55 mm) respectively The duct ensures that all the fins sides were exposed to the air flow. The piezoelectric fan is equivalent to the MIDE technology product type PFN – 1011 as shown in **Fig. 2,** and its properties are shown in **Table 1.**

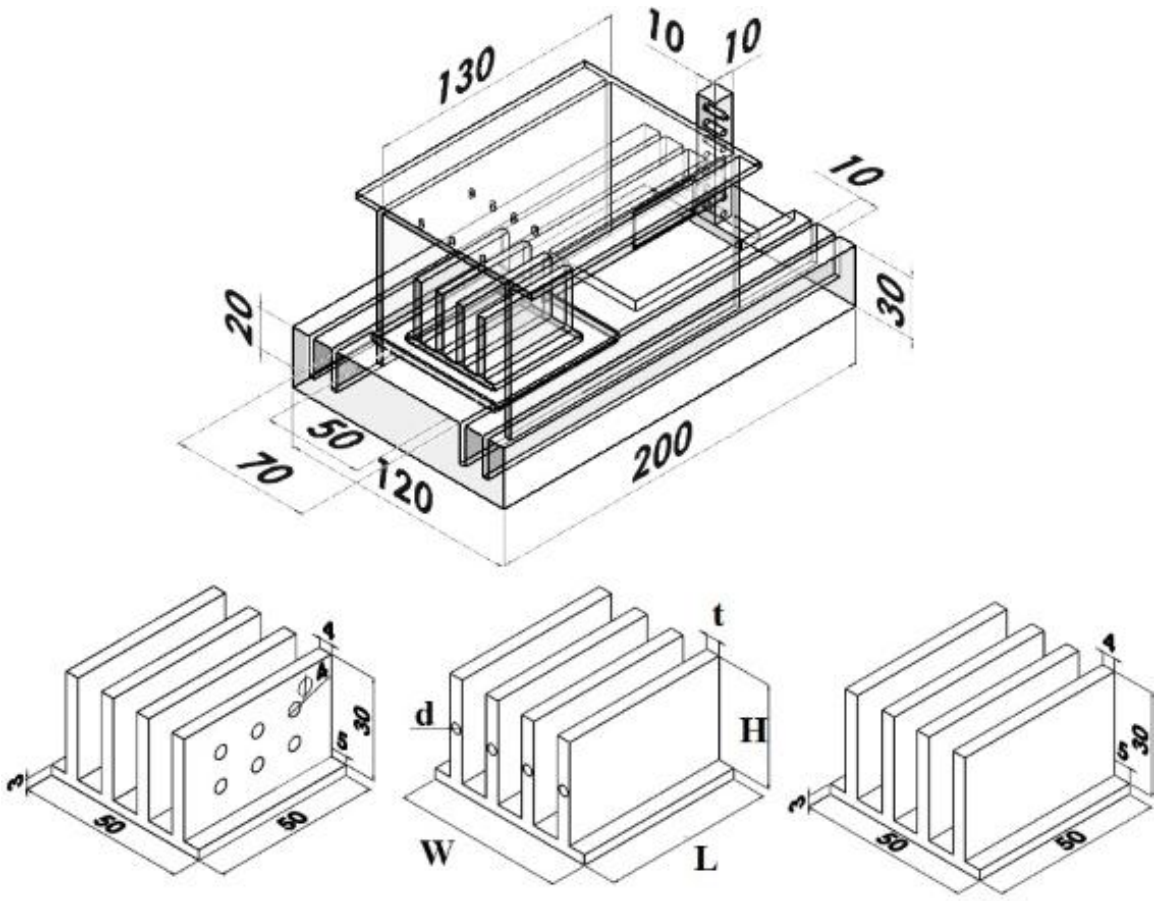


**Figure 1.** Solid and perforated finned heat sink with schematic drawing for the test Rig, all dimensions are in (mm).

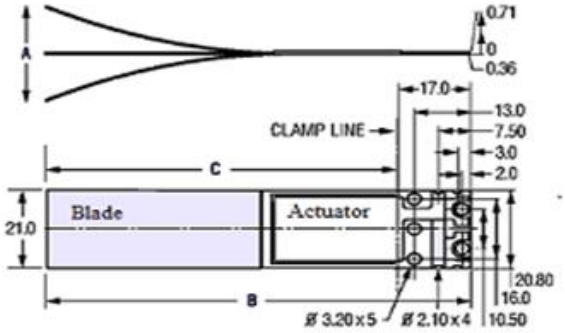


| | PFN-1011 | PFN-1012 |
|---|---|---|
| A (mm) | 40 | 28 |
| B (mm) | 103.5 | 97 |
| C (mm) | 86.5 | 80 |

**Figure 2.** Piezoelectric fan dimensions, all dimensions are in (mm).

**Table 1.** Piezoelectric fan specification.

| Specification | PFN-1011 |
|---|---|
| Static Pressure @Max. Voltage | 25 Pa |
| Max Flow rate @ Max. Voltage | 10.2 CFM |
| Capacitance | 27 µF |
| Resonant Frequency ($f_n$) @85 C | 50 +/-1 Hz |
| Max Voltage | 240 VAC RMS |
| Current at $f_n$ at Max Voltage | 3.2 mA |
| Power at $f_n$ at Max Voltage | 0.77 W |
| Displacement at Max Voltage | 40 mm |
| Max Current | 10 mA |
| Mass | 2.9 g |

### 2.1 Boundary Conditions

The air flow considered to be steady and turbulent with constant properties. The airflow is generated by piezoelectric fan; the flow behavior fluctuates due to piezoelectric fan characteristics. The piezoelectric fan is fluctuating from side to another with harmonic motion and frequent 50 times per second. Furthermore, its position is eccentric relative to the duct. So, it's not possible to consider the inlet velocity as constant to solve this problem the inlet area of the duct divided to velocity contour as shown in **Fig. 3**, these values are measured experimentally by a hot wire anemometer device type AM - 4214 for each heat sink at three piezoelectric fan amplitudes (25 mm, 30 mm, and 40 mm). The ambient temperature considered 37 ℃ as it measured in the laboratory during summer. To simulate the electronic devices conditions, the heater power considered to be 10.85 watt that produced a constant heat flux 4340 W/m$^2$ exposed to the base of the heat sink.

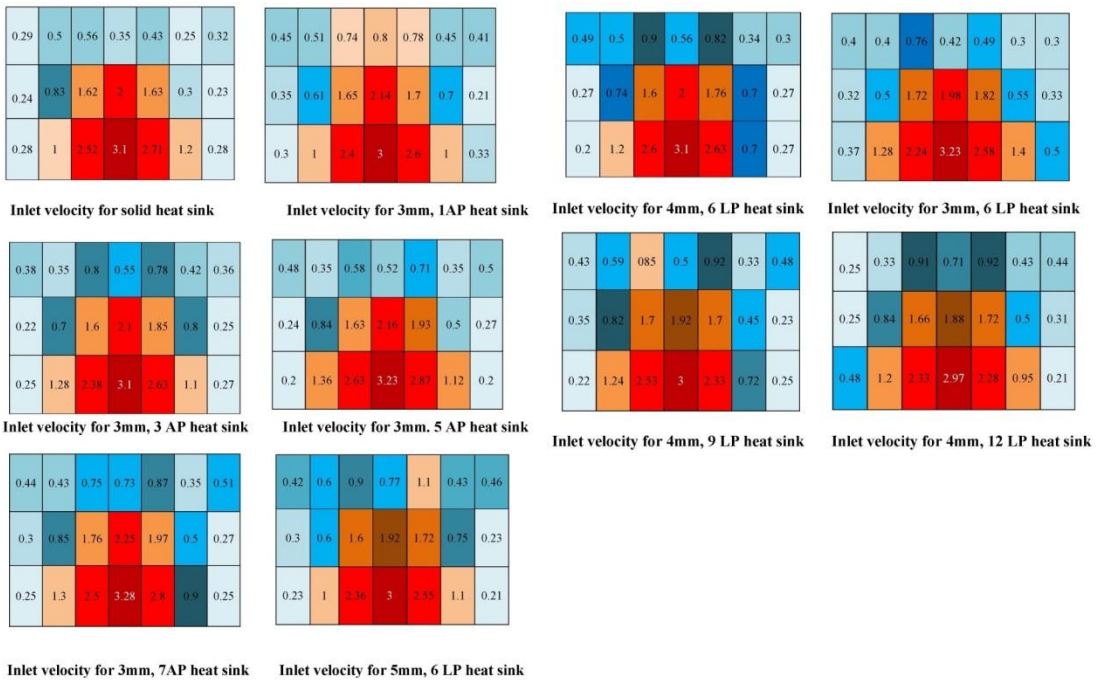


**Figure 3**. Velocity contour for solid and perforated heat sinks, all data are in (m/s).

## 2.2 The Domain

**Fig. 4**. Shows the working domain, this domain consists of inlet which is starts from the piezoelectric tip where the velocities are measured and its end representing the Perspex duct exit. Its dimensions are 52 mm in length, 70 mm in width, and 55 mm in height, where the gap between the fins and the fan tip is one mm. The flow is moved around fins and through the perforations also the base surfaces that exposed to the flow, because of immersing of the heat sink base in the Teflon base.

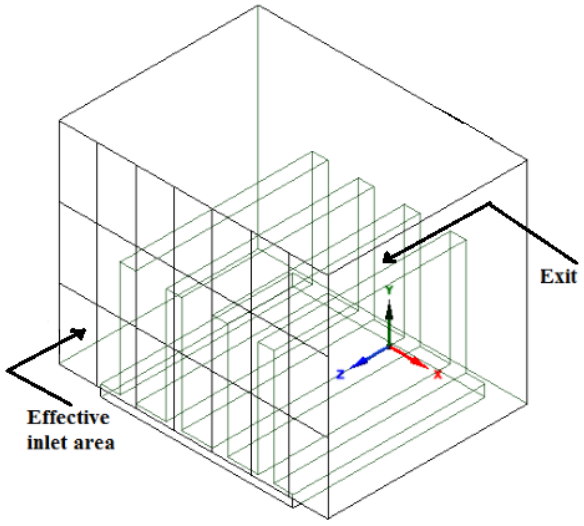


**Figure 4.** Solid and fluid domain with 21 velocity inlets.

The inlet is divided into 21 inlet zone and fed with air velocity values that measured experimentally all these values are measured three times, for each finned heat sinks sample and piezoelectric fan amplitude.

## 3. THE GOVERNING EQUATIONS

### 3.1 Flow and Energy Equations

The general three-dimensional steady state incompressible flow Ansys workbench 17.2 governing equations are:

Continuity equation: $\frac{\partial}{\partial x_i} u_i = 0$ (1)

Momentum equation: $u_j \frac{\partial u_i}{\partial x_j} = -\frac{1}{\rho}\frac{\partial P}{\partial x_i} + v\frac{\partial^2 u_i}{\partial x_i^2}$ (2)

Energy equation: $u_j \frac{\partial T}{\partial X_j} = \alpha \frac{\partial^2 T}{\partial X_i \partial X_j}$ (3)

Where $x_i$ and $x_j$ are tensor forms in the *i*th and *j*th direction ($i = j = 1, 2 = x, y$), $u_i$ and $u_j$ are the set-mean velocity tensors and $p$ is the pressure of the air. $\rho$ Is the density of the air, assumed incompressible flow, and $v$ kinematic viscosity are constant values.

### 3.2 The Time-Averaged Equations

To solve and chose the three-dimensional governing equations package, the flow considered as steady state, incompressible fluid flow, and turbulent, and modeled with RNG k - ε with swirl and scalable wall function are the same as used by **Velayati,** and **Yaghoubi, 2005.** Applied the time-averaging procedures to preservation equations, the equations that rules the mean-flow quantities, $u_i$, p and T, for turbulent flow are:

$$u_{i,j} = 0 \quad (4)$$

$$\rho(u_j u_{i,j}) = -Pi + |\mu(u_{i,j} + u_{j,i}) - \rho u'_i u'_j| \quad (5)$$

$$\rho C_p(u_j T_j) = (\lambda T_j - p C_p u'_j T')_j \quad (6)$$

Applying the Boussinesq approximation, the Reynolds stress tensor and turbulent heat fluxes are:

$$-\rho u'_i u'_j = 2\mu_i S_{i,j} - \frac{2}{3}\rho k \delta_{ij} \quad (7)$$

$$-\rho C_p u'_i T' = \lambda_i T_j \quad (8)$$

### 3.3 The RNG Based k– ε Turbulent Model

k– ε models deals with boundary layers separation and reattachment, otherwise re-circulation than the standard k– ε model. **Yakhot,** and **Orszag, 1986,** proposed a variant of the k–ε model such that its performance characteristics were improved relative to the standard model. Neglecting buoyancy the k and ε equations of the RNG model effects are as below:

$$\rho u_j k_j = ((\mu + \frac{\mu_t}{\sigma_k}) k_j)_j + G - \rho\varepsilon \quad (9)$$

$$\rho u_j \varepsilon_j = ((\mu + \frac{\mu_t}{\sigma_\varepsilon}) \varepsilon_j)_j + c_1 \frac{\varepsilon}{k} G - \frac{c_\mu \eta^3 (1 - \eta/\eta_0)}{1 + \beta\eta^3} \frac{\varepsilon^2}{k} - c_2 \rho \frac{\varepsilon^2}{k} \quad (10)$$

The shear generation and viscous dissipation of $\varepsilon$ represented by the terms $c_1 \frac{\varepsilon}{k} G$ and $c_2 \rho \frac{\varepsilon^2}{k}$ as shown in eq. (10). Where $c_1$ = 1.42, $c_2$ = 1.68 are coefficients in turbulence

model. The additional term in the above equation induct the parameter η. The ratio of characteristic time scales of turbulence and the mean flow fields is defined by η = Sk /$\varepsilon$ , $\eta_o$ = 4.38 and it can be written as shown below:

$$\eta = \sqrt{c_\mu^{-1}(G / \rho\varepsilon)} \quad \text{, Where } c_\mu = 0.085 \tag{11}$$

**3.4 Solution Procedure**

Solving conduction equation for thermal zones, as the finned heat sinks field is calculate with set of equations. The surface area of the finned heat sinks can be calculated by using the below equations:

**a- solid fin**

$$A = WL + N_f\,[2Ht_{fin} + 2HL + Lt_{base}] \tag{12}$$

**b- axial perforated fins**

$$A = WL + N_f\,[2HL + 2(Ht_{fin} - \pi/4d^2N_P) + \pi dLN_p + Lt_{base}] \tag{13}$$

**c- axial perforated fins**

$$A = WL + N_f\,[2HL + 2(Ht_{fin} - \pi/4d^2N_P) + \pi dLN_p + Lt_{base}] \tag{14}$$

The overall heat transfer coefficient at the heated wall can be calculated from the convectional heat transfer equation:

$$Q_N = h_{av}A[T_w - T_f] \tag{15}$$

Then, the overall heat transfer coefficient can be written:

$$h_{av} = \frac{Q_N}{A(T_w - T_f)} \tag{16}$$

$$T_f = \frac{T_b + T_{in}}{2} \tag{17}$$

$$\dot{m} = \sum_{i=1}^{21} \rho A_d V_a \tag{18}$$

But the area and the density considered constant. Thus:

$$\dot{m} = \rho A_d \sum_{i=1}^{21} V_a \tag{19}$$

Calculation of the fins effectiveness for any fin is extremely important to determine fin thermal performance for multi porosities. "Although the installation of fins will alter the surface convection coefficient, this effect is commonly neglected. Hence, assuming the convection coefficient of the finned surface to be equivalent to that of the un-finned base" **Frank, 2011**. Thus, the effectiveness (£) is the percentage ratio of the net fins heat

transfer rate ($Q_f$) to the maximum heat transfer rate the same heat sink but without the fins ($Q_{max}$) at the base temperature as in the equation

$$£ = \frac{Q_f}{Q_{max}} \quad (20)$$

## 4. THE COMPUTATIONAL SCHEME DOMAIN

### 4.1 Geometry Description and Mesh Domain

The domain is illustrated in **Fig. 4**. The inlet side represents the piezoelectric fan tip position, it is illustrated 0.5 mm in front of the finned heat sink and the exit side represents the flow out let at the end of the duct. The inlet mesh contains 21 velocity inlets. Both upper and sides surfaces are represents the duct walls respectively**.** The duct sides are 10 mm spaced far from the fins sides to allow the air induced through the side gaps avoid the adiabatic walls, that's make the results more realistic and 25mm between duct surface and fin tips. Due to piezoelectric fan range and previous studies, the computational domain is chosen. The generations of appropriate mesh elements in the three dimensions by using Ansys 17.2. Meshing is so bushy near the fin surfaces and perforation walls to get more accurate values. The number of mesh element will defer from sample to another because of different number of perforations and its sizes. For axial perforation a three perforated finned heat sink chosen as sample, in lateral for increasing the window size the 5mm perforation defined as sample from its group, and for increasing the perforations number 4mm hole diameter nominated as sample in this study as shown in **Table 2**.

**Table 2.** Mesh generated for finned heat sinks and fluid domain.

| No. | Type | No. and size of perforations | Finned Heat Sink Mesh | All Domain Mesh |
|---|---|---|---|---|
| **1** | Solid | 0 | 262843 | 808012 |
| **2** | AP | 3 with 3 mm | 422547 | 1003938 |
| **3** | LP | 6 with 5 mm | 390382 | 499358 |

The mesh configuration for perforated fin with three perforations is shown in **Fig. 5**. The solution is performed by changing piezoelectric fan amplitude in three speeds and repeats it for each finned heat sink and average heat transfer coefficient and effectiveness is determined**.**

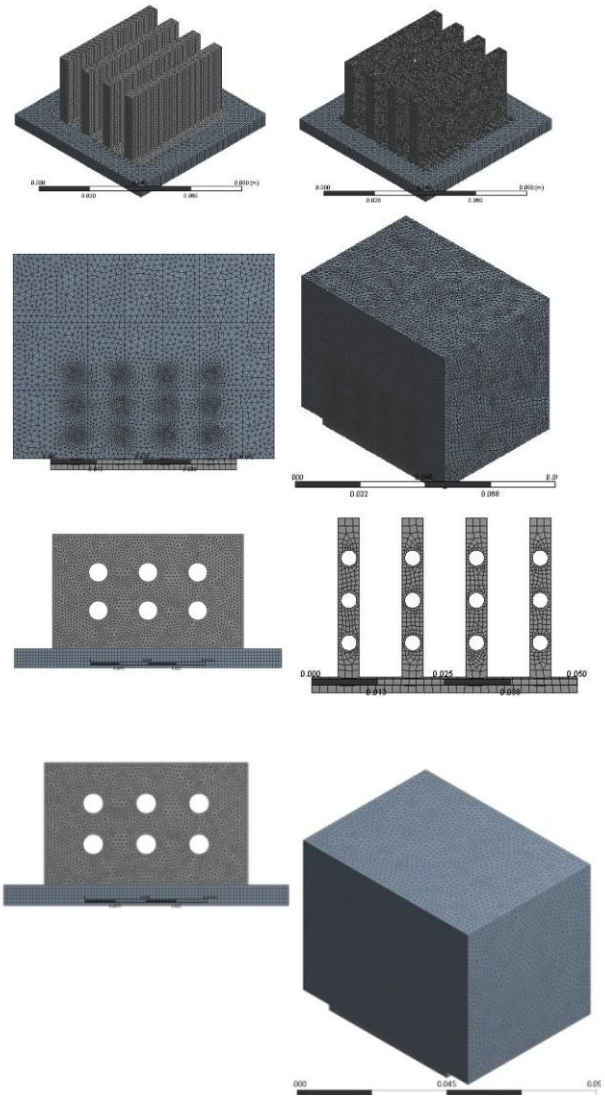

**Figure 5**. Typical grid configurations for flow domain and perforated finned heat sinks.

### 4.2. The Procedure

A SIMPLE algorithm which developed by **Patankar, 1980** is discretize the governing equations by the finite volume method. Using the discretization scheme cells of the control volume (the velocity components) is tottered relatively to the main control volume cells. The first order upwind technique is used to calculate velocity components, k‹ and ε with swirl dominate flow and energy equations. In Ansys workbench 17.2, fluent solver is used after designing the model of the finned heat sink by Ansys workbench 17.2. The solution proceeds as following: Generate both the geometry, Boolean and define the target and tools domains**.** Define all the boundary surfaces then generate the mesh of the domain, **Table 2** shows samples of mesh number for three different heat sinks**.** Setup the heat source, define the inlet velocities, define out let mass flow rate, define the heat flux and heat transfer coefficient**.** Specify the properties of the fluid used such as air density and viscosity and boundary conditions. Define the RNG k-ε solution method of problem with simple scheme with 0.1 relaxations for all parameters**.** Initialize hybrid solution and run calculations**.** Steady state temperatures are calculated**.** Analyze the problem after specifying the convergence criteria which is $10^{-4}$, and the iterations

number**.** The iteration number is the maximum number of repeated computations done before the solver finishes. As in the present case, 36000 iterations are requested depending on the domain and mesh sizes. The cases of the present work that have been tested in Ansys workbench 17.2 fluent solver are 30 cases depending on the variation in perforations and piezoelectric fan amplitude.

Ansys workbench 17.2 contains a number of solvers for partial differential equations (PDE)-based problems. The present work used a stationary to solve PDE problems which were presented for linear and nonlinear problems. The stationary steps were split into sub steps Newton method with only Jacobean related components are dependent procedure in this method of solution which can save both memory and time to solve. For the steady RNG k-ε simulations, the initial inlet conditions were used to initialize the flow, and the solution was iterated till the convergence is achieved.

### 4.3 Code Validation

For the model variation of piezoelectric fan amplitudes with both solid and axial perforated fins of the present study, to the best of the authors' knowledge there is not similar experimental or numerical investigation. But for axial perforated heat sinks **Shaeri,** and **Yaghoubi, 2009,** studied numerically the turbulent convection heat transfer from an array of perforated fins; the general behavior of increasing the number of perforations increases the effectiveness of the perforated fins compared with solid fins as shown in **Fig. 6**. For lateral the results agreed with an experimental work "Heat transfer analysis of lateral perforated fin heat sinks" by **Shaeri,** and **Yaghoubi, 2009,** they found that the fins with the same number of perforation but larger windows have higher Nu number than the smaller windows. Also the fins with higher number of perforations per fin have other advantages lower weight, lower drag force, and higher heat transfer as shown in **Fig. 7**. These results have good agreement with the present study.

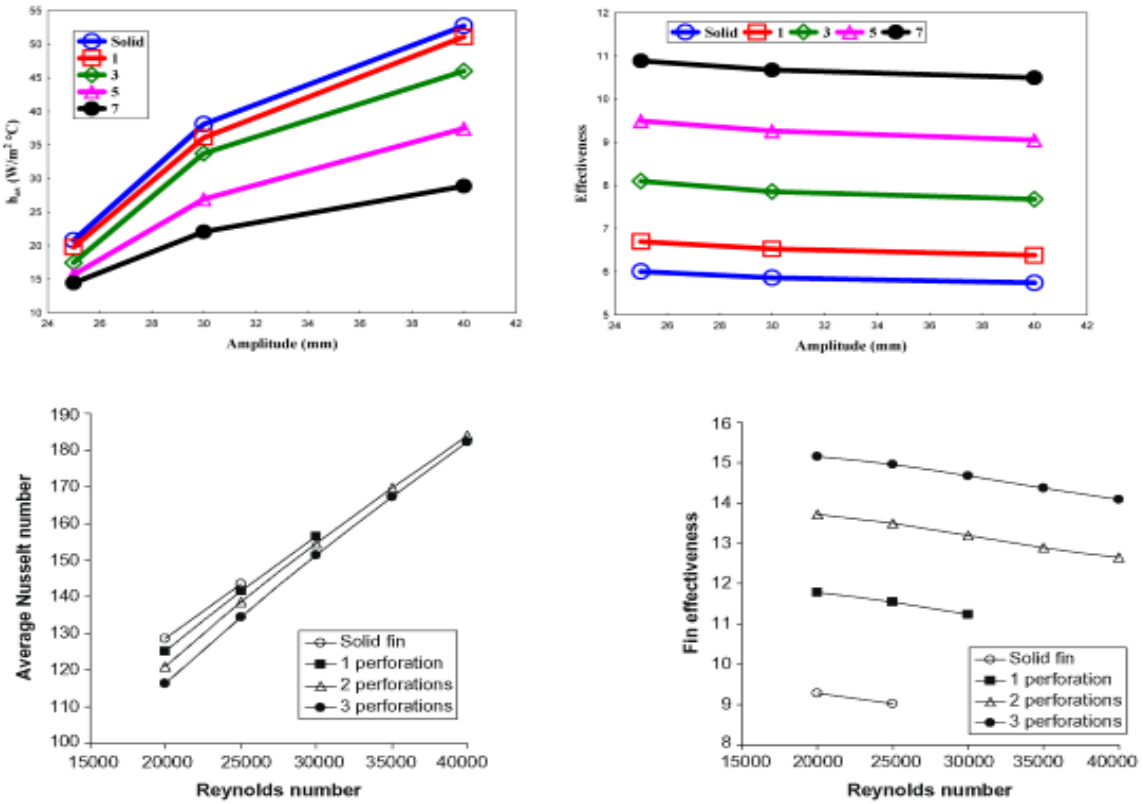


**Figure 6**. General behavior for numerical AP heat sinks in previous and present work.

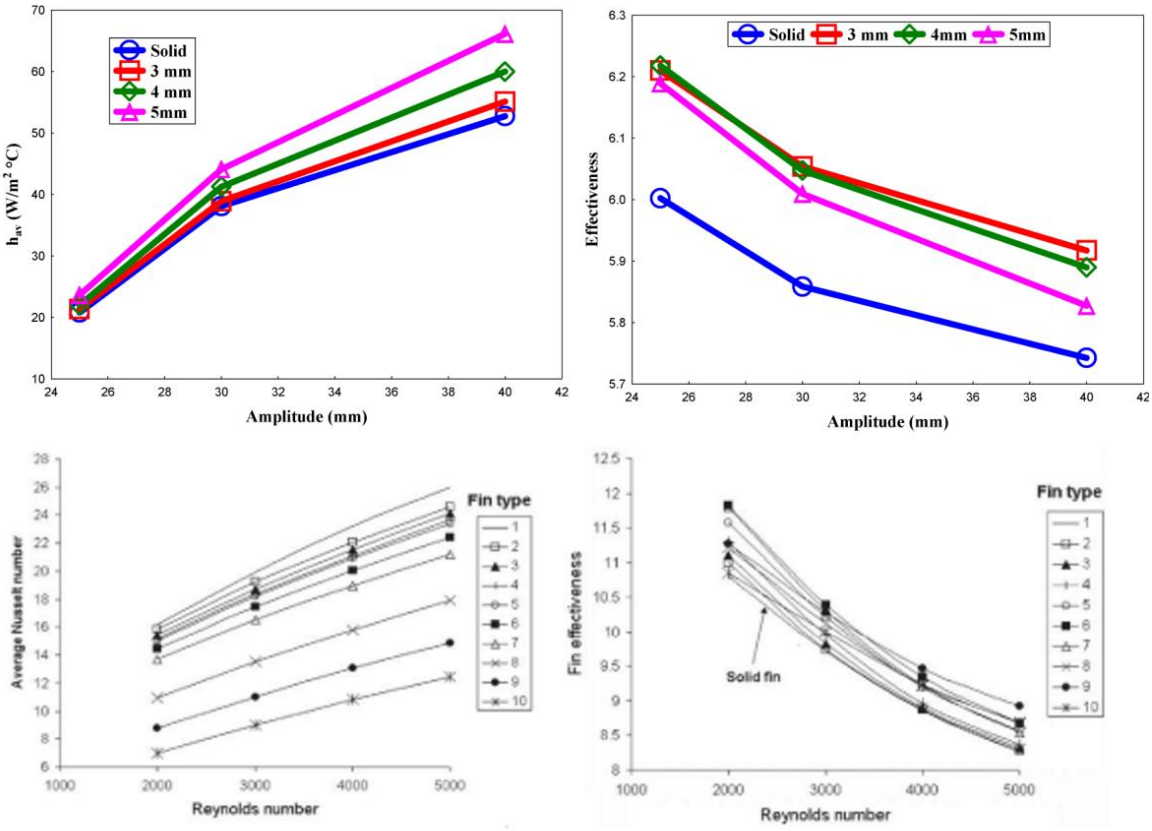


**Figure 7.** General behavior for experimental LP heat sinks in previous and present work.

## 5. RESULTS AND DISCUSSION

### 5.1 The Temperature Distribution

The main goal of the numerical study is to simulate the heat transfer and the air flow characteristics in order to deduce information about the temperature distribution in both free and forced convection and streamlines. The free convection solution (transient zone) is produced the solid and the 3 axial perforation finned heat sink only but the flow zone or piezoelectric fan ON zone is produced for solid, 3mm three axial perforated, and 5 lateral perforated finned heat sinks.

**Fig. 8** shows the temperature contour of applying a constant heat flux of 4340 W/m$^2$ on the solid heat sink; also its shows the temperature distribution through the finned heat sink. The heat is conducted from the base towards fins. The base temperature is higher than the fins temperatures due to free convection. And the central fins temperature is higher than the lateral due to the lateral fins are composed to the free stream from one side this will help the fins to exchange the heat with the free stream.

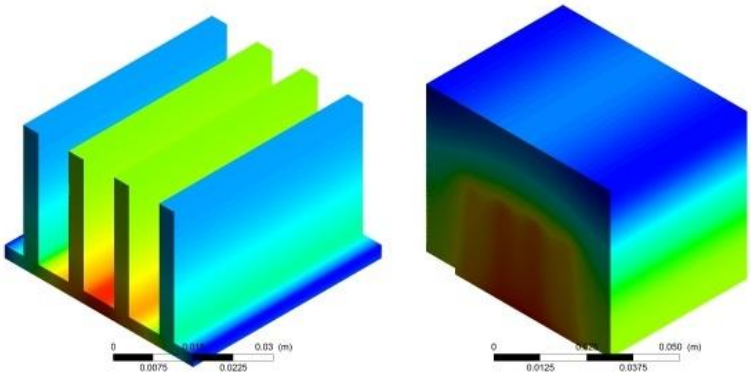

**Figure 8**. 1st Steady state temperature and heat distribution in solid finned heat sink exposed to constant heat flux 4340 W/m$^2$.

**Fig. 9** shows the second steady state temperature distribution for the solid finned heat sink after allowed the piezoelectric fan to work for half hour. The flow generated is oscillates from minimum to maximum values and changing its direction from side to another this will cause a swirl and turbulent in the flow this will affected on temperature distribution and the heat dissipation from the finned heat sink.

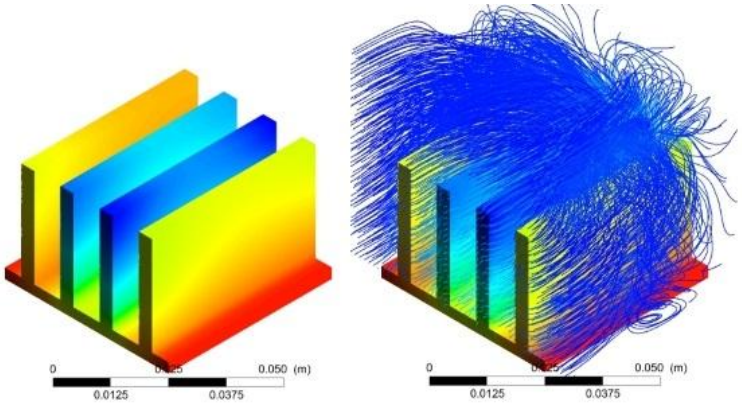

**Figure 9.** 2nd Steady state temperature and flow behavior for solid finned heat sink with piezoelectric fan amplitude 40mm.

The central fins will have the decreased temperatures because of the biggest amount of air flow will crossed through the heat sink. Also increasing the fan amplitude will decrease the average steady state temperature. **Fig. 10** shows the effect of applying a constant heat flux 4340 W/m$^2$ on a three axial perforated (AP) finned heat sink, when piezoelectric fan OFF. It can be observed that the heat distributed equally through the fins, this is due to the perforation in each fin. These perforations help the flow crossing the fins causing better heat transfer from the base to the fin tips.

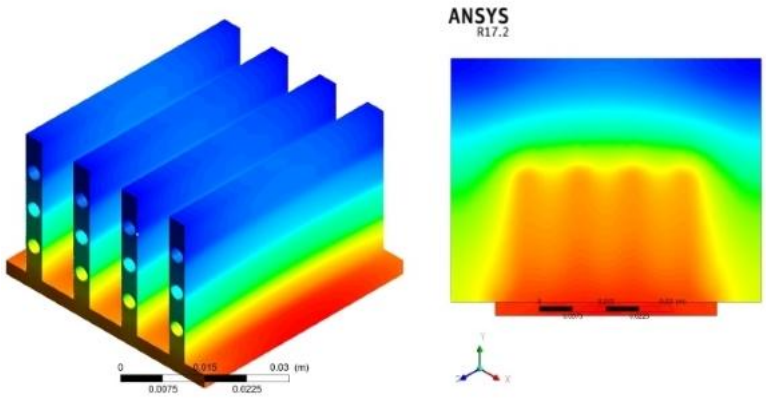


**Figure 10.** 1st steady state temperature and dissipated heat to the duct zone at transient zone for AP finned heat

At the 2nd Steady State Zone [Piezoelectric Fan ON], **Fig. 11** shows the temperature distribution for the 3 AP finned heat sink. The temperature distribution shows the behavior of heat dissipation from the finned heat sink where the internal fins is dissipated heat faster than the external fins due to the amount of air that crossing the heat sink and the perforations.

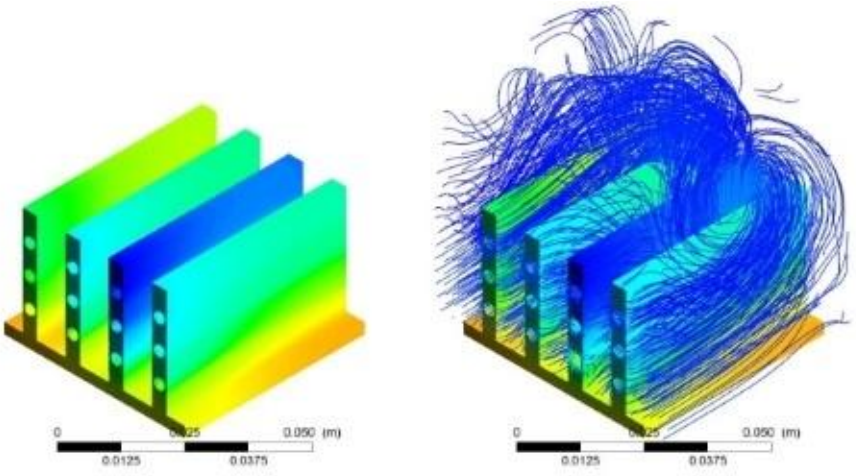

**Figure 11**. 2nd steady state temperature and flow stream lines generated by piezoelectric fan with amplitude 40 mm to the 3AP finned heat sink.

**Fig. 12** shows the temperature distribution of a 5 mm with six lateral perforated finned heat sink which its exposed to a constant heat flux and air flow that generated by a piezoelectric fan with amplitude 40 mm. It seems the temperature distribution through the LP fins contour is decreased compared with the solid one and it can be observed that the perforation helped the air to cross through the fins and decreased the average temperature of the heat sink.

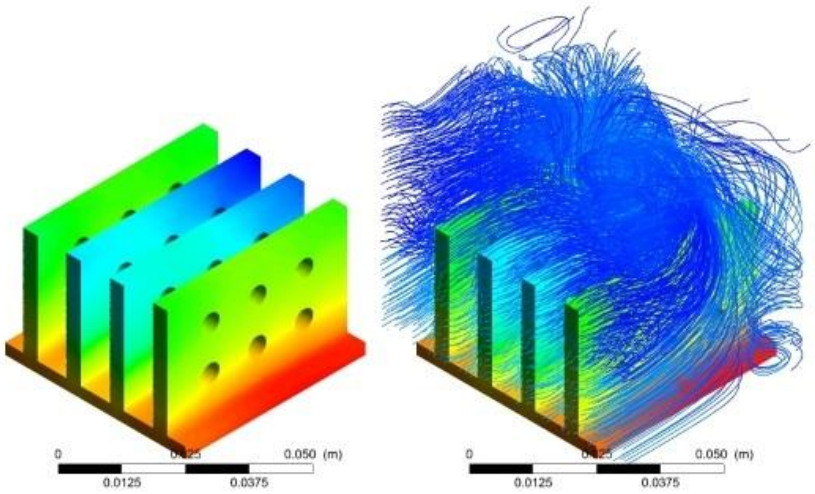


**Figure 12.** 2nd steady state temperature for lateral perforated finned heat sink after running the piezoelectric fan with 40 mm tip amplitude.

### 5.3 The Heat transfer Coefficient

**Fig. 13** shows the variation of the coefficient of heat transfer values with amplitude for both solid and axial perforated finned heat sinks which they exposed to heat flux 4340 W/m$^2$ and piezoelectric fan with amplitude (25 mm, 30 mm and 40 mm). A general behavior can be deduced that the values of the average heat transfer coefficient are highly affected by the piezoelectric fan amplitude and increased when the fan amplitude is increased. It can be noted that the heat sink with higher number of perforations exhibit a lower average heat transfer coefficient values. This can be attributed to the reduction in the diffused energy from the heat sink base towards the fin tip for higher number of perforations.

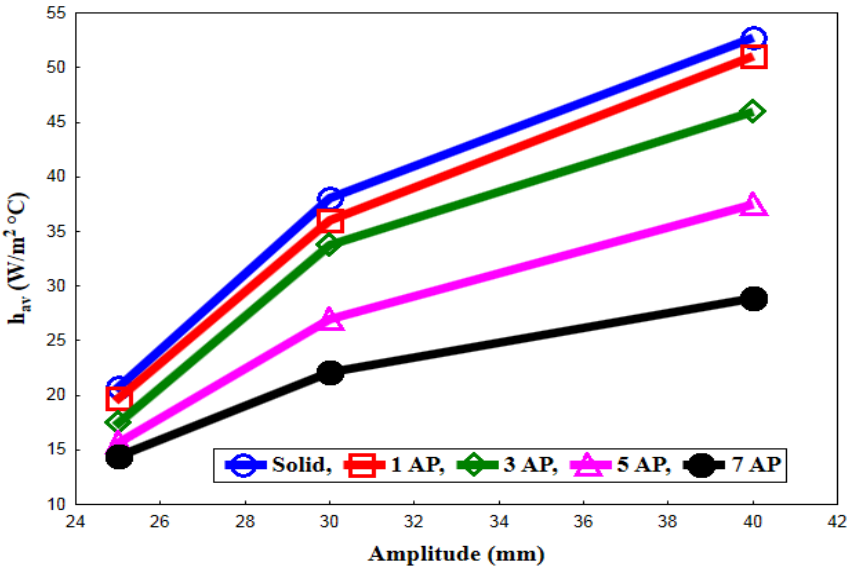


**Figure 13.** Average heat transfer coefficient variation for the solid and axial perforated finned heat sinks.

**Fig. 14** shows the variation of the coefficient of heat transfer values with amplitude for both solid and six different size lateral perforated finned heat sinks. A general behavior can be seen that the values of the average heat transfer coefficient are increased when the fan amplitude is increased. It can be noted that increasing perforation size will increase the heat transfer coefficient; this behavior is due to the windows that increased the turbulent around the fins which enhanced the heat transfer from perforated fins compared with solid fin**.**

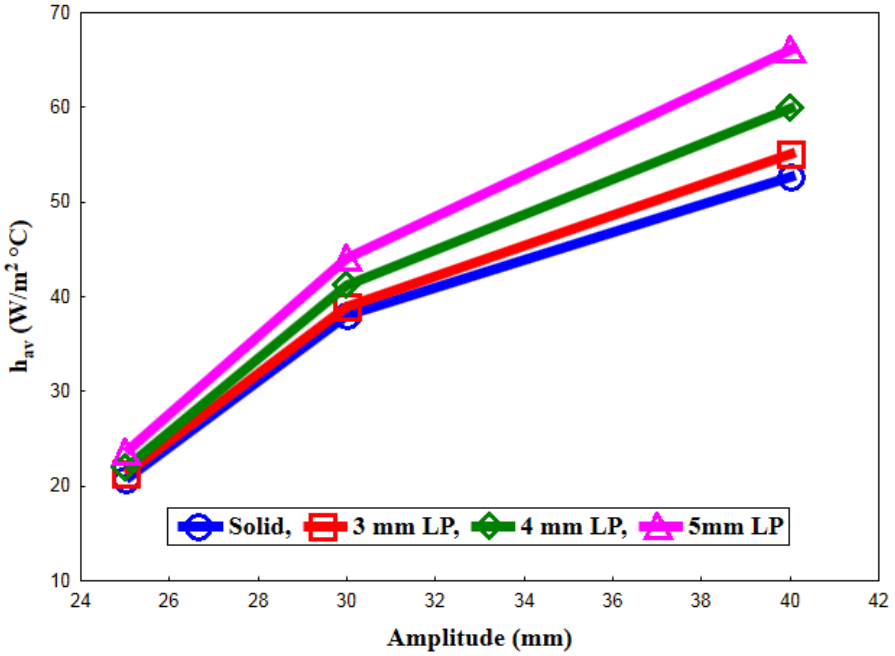


**Figure 14.** Average heat transfer coefficient variation with piezoelectric fan for solid and lateral perforated heat sink with different holes size.

**Fig. 15** shows the variation of the coefficient of heat transfer values with amplitude for both solid and 4 mm different number of LP finned heat sinks which they exposed to heat flux 4340 W/m$^2$ and piezoelectric fan with amplitude (2.5 cm, 3.0 cm and 4.0 cm). When the fan amplitude increased the coefficient of heat transfer values are also increased. Another observation can be deduced from **Fig. 13** that as the number of perforations increased to a certain number (six perforations), the values of the coefficient of heat transfer are increased. But for higher number of perforations, the coefficients of heat transfer values are decreased due to the reduction in the heat diffusion from the heat sink base.

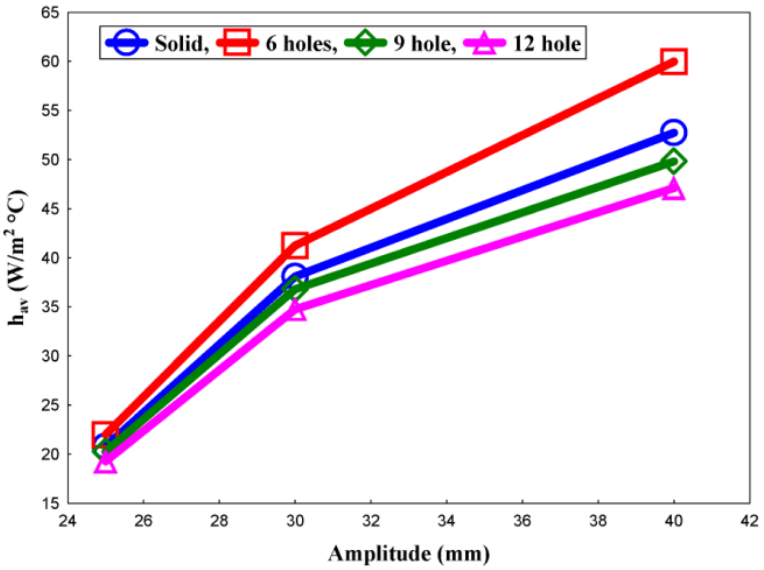


**Figure 15.** Average heat transfer coefficient variation with piezoelectric fan amplitude for solid and lateral perforated heat sink with different number of perforations

**Fig. 16** shows the variation of the effectiveness values with amplitude for both solid and axial perforated finned heat sinks. A general behavior can be deduced that the values of the average effectiveness are affected by the piezoelectric fan amplitudes and decreased when the fan amplitude is increased. It can be noted that the heat sink with higher number of perforations exhibit a higher effectiveness values

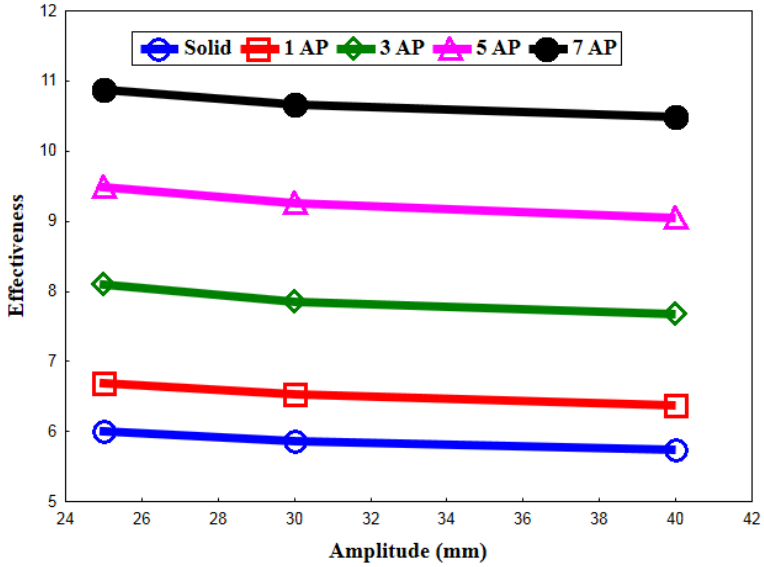


**Figure 16.** Effectiveness variation with piezoelectric fan amplitudes for the solid and perforated finned heat sinks

**Fig. 17** shows the behavior of numerical results of effectiveness with piezoelectric fan with amplitude (25 mm, 30 mm and 40 mm) for solid and 6 LP finned heat sinks which they exposed to heat flux 4340 W/m$^2$. It can be observed that the effectiveness will decrease with both increasing the holes size and increasing the fan amplitudes.

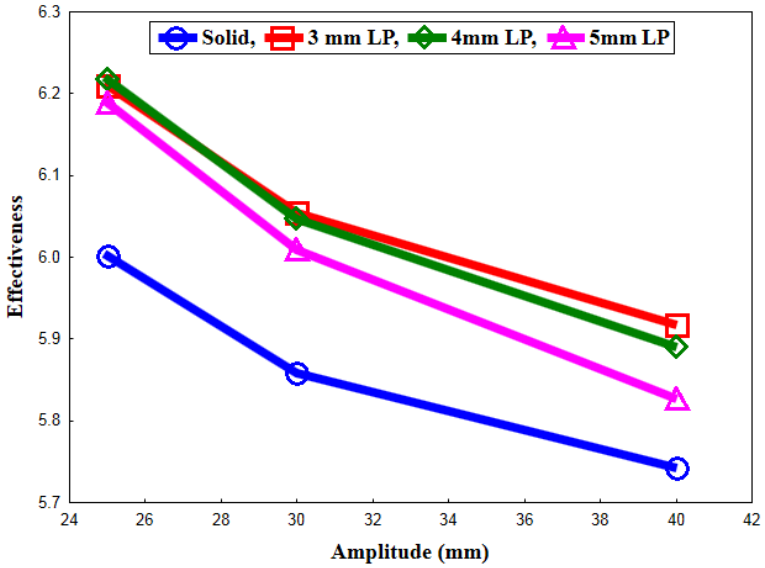


**Figure 17.** Effectiveness variation with piezoelectric fan tip amplitude (2.5 cm, 3.0 cm, 4.0 cm) for lateral perforated heat sink with different holes.

**Fig. 18** shows the behavior of numerical results of effectiveness with piezoelectric fan with amplitude (25 mm, 30 mm and 40 mm) for solid and 4mm LP finned heat sinks group which they exposed to heat flux 4340 W/m$^2$. It can be shown increasing the number of perforations will increase the effectiveness but increasing fan amplitude will decrease the effectiveness.

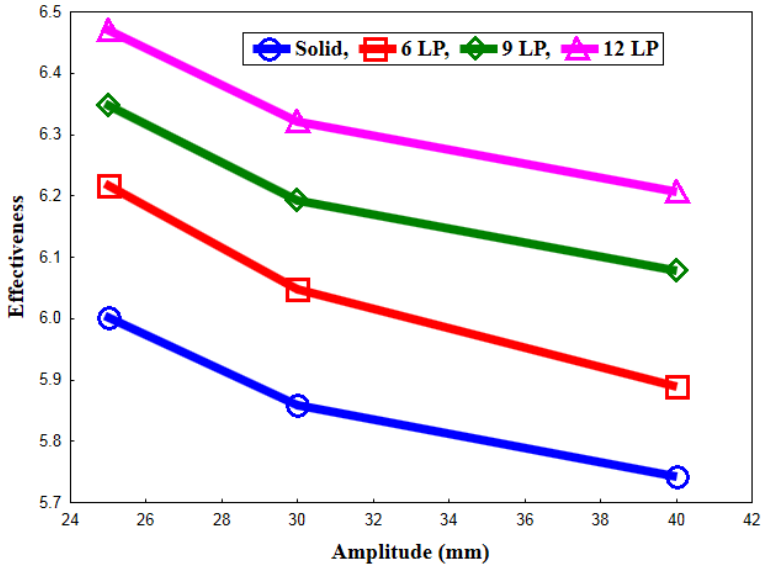


**Figure 18.** Effectiveness variation with piezoelectric fan amplitude for solid and lateral perforated heat sink with different number of perforations.

## 6. CONCLUSIONS

1. Using perforation may enhance the heat dissipation.
2. Increasing in axial and lateral perforations number will increase the temperature difference between the base temperature and fin tip.

3. The heat transfer coefficient for axial and lateral perforations will increased with increasing the piezoelectric fan amplitudes to the maximum value.
4. Heat transfer coefficient with axial and lateral perforations will decrease with increasing number of perforations.
5. The heat transfer coefficient with lateral perforations will increase with increasing the size of perforations.
6. Effectiveness with axial perforations will be decrease with increasing of piezoelectric fan amplitudes and increase with increasing perforations.
7. Fins effectiveness will decrease with increasing the piezoelectric fan Amplitudes with both axial and lateral perforations.

## 7. REFERENCES


- Acikalin, A. Raman, and Garimella S. V., 2003, *Two-dimensional streaming flows induced by resonating thin beams,* J. *Acoustical Society of America*, vol.3, pp. 1785-1795.
- Acikalin, S.M. Wait, S.V. Garimella, A. Raman, 2004, *Experimental investigation of the thermal performance of piezoelectric fans,* J. Heat Transfer Eng. Vol. 25 p.p. 4–14.
- AIEssa A.H., Maqableh A.M., Ammourah S., 2012, *Augmentation of Fin Natural convection heat dissipation by square perforations.* J. Mech Eng Automat, vol. 2, p.p. 1–5.
- Dorignac E., Vullierme J.J., Broussely M., Foulon C., Mokkadem M., 2005 *Experimental heat transfer on the windward surface of a perforated flat plate*. Int. J. Therm Sci. vol. 44, p.p. 885–93.
- Incropera, F.P., and DeWitt, D.P., 2011 *Introduction to Heat Transfer* third ed., John Wiley & Sons, Inc.
- Kavita H. Dhanawade, Vivek K. Sunnapwar, and Hanamant S. Dhanawade, 2016, *Optimization of Design Parameters for Lateral Circular Perforated Fin Arrays under Forced Convection*. J. Heat Transfer—Asian Research, vol. 45 (1), p.p. 30-45.
- Kimber, M., Garimella, S.V. and Raman, A., *2007, "Local heat transfer coefficients induced by piezoelectrically actuated vibrating cantilevers*", Journal of Heat Transfer, Vol. 129, pp. 1168–1176.
- Patankar, S.V., 1980, Numerical Heat Transfer and Fluid Flow. Hemisphere, Washington, DC.
- Petroski, M. Arik, M. Gursoy, 2010, *Optimization of piezoelectric oscillating fancooled heat sinks for electronics cooling*, IEEE Trans. Compon. Packag. Technol. Vol. 33, p.p. 25–31.
- Sahin, B, and Demir, A., 2008 *Performance analysis of a heat exchanger having perforated square fins*. J. Appl Thermal Eng, vol. 28, p.p. 621–632.
- Sara ON, Pekdemir T, Yapici S, Ersahan H. 2001, *Heat transfer enhancement in a channel flow with perforated rectangular blocks*. Int. J. Heat Fluid Flow, vol. 22, p.p. 509–18.
- Shaeri MR, and Yaghoubi, M., 2009, *Heat transfer analysis of lateral perforated fin heat sinks*. j. Applied. Energy, vol. 86, p.p. 2019–2029.
- Shaeri, M.R., and Yaghoubi, M., 2009, *Numerical analysis of turbulent convection heat transfer from an array of perforated fins*, Int. J. Heat and Fluid Flow, vol. 30, p.p. 218–228.

- Torii, S. and Yang, W.J., 2002, *Thermal transport phenomena over a slot-perforated flat surface in pulsating free stream*. Int. J. Therm. Sci. 41, p.p. 241–52.
- Velayati, E., and Yaghoubi, M., 2005, *Numerical study of convective heat transfers from an array of parallel bluff plates*. Int. J. Heat Fluid Flow, vol. 26, p.p. 80–91.
- Wadhah Hussein Abdul Razzaq AI-Doori, 2011, *Enhancement of natural convection heat transfer from the rectangular fins by circular perforations*, International journal of automotive and mechanical engineering, vol.4, pp. 428-436.
- Yakhot, V. and Orszag, S.A., 1986, *Renormalization group analysis of turbulence*. J. Sci. Comput. Vol. 1, p.p. 3–51.


## 8. NOMENCLATURE

| Letter | Description | Units |
|---|---|---|
| $A$ | Heat Sink Surface Area | $m^2$ |
| $A_d$ | Effective Cross Sectional Area of the Duct | $m^2$ |
| $d$ | Diameter of Perforation | m |
| $h_{av}$ | Heat Transfer Coefficient | W/ ($m^2$. K) |
| $H$ | Fin Height | m |
| $L$ | Length | m |
| $\dot{m}$ | Mass Flow Rate | $m^3$/s |
| $N_{fin}$ | Number of Fins | - |
| $N_P$ | No. of Perforations | - |
| $Q_f$ | Heat Transfer From Finned Heat Sink | W |
| $Q_{max}$ | Heat Transfer From No Finned Heat Sink | W |
| $Q_N$ | Net Heat transfer | W |
| $t_{base}$ | Heat Sink Base Thickness | m |
| $t_{fin}$ | Fin Thickness | m |
| $T_b$ | Bulk Temperature | ℃ |
| $T_f$ | Film Temperature | ℃ |
| $T_{in}$ | Ambient Temperature | ℃ |
| $T_w$ | Wall Temperature | ℃ |
| $u_i$ | Index Notation of Velocity Components | m/s |
| $u'u_j$, $u'T'$ | Turbulent Reynolds Stress Tensor and Heat Flux | - |
| $V_a$ | Air Velocity | m/s |
| $W$ | Width | m |

| Letter | Description | Units |
|---|---|---|
| $\alpha$ | Fluid Thermal Diffusivity, Angle of Attack | $m^2/s$ |
| $\beta$ | Parameter in RNG *k*- ε Mode, 0.012 | - |
| $\delta_{ij}$ | Kronecker Delta Function | - |
| ε | Turbulent Dissipation Rate, $\mu(u_{ij}u_{ij})/\rho$ | - |
| η | Parameters in RNG *k*- ε Mode, *Sk*/ ε | - |
| $\lambda_1\lambda_2$ | Total and Turbulent Thermal Conductivity of Fluid,( $\lambda_0$ + $\lambda_1$) , $(Cp\mu/\sigma t)$ | - |
| $\lambda_0$ | Laminar Thermal Conductivity of Fluid | - |
| $\mu, \mu_t$ | Total and Eddy Viscosity, ( $\mu + \mu_t$), $(c_\mu \rho k^2/ \varepsilon)$ | - |
| $\mu_o$ | Laminar Viscosity | kg/m s |
| $\rho$ | Density | $kg/m^3$ |
| £ | Effectiveness | - |

| SYMBOL | DESCRIPTION |
|---|---|
| AP | Axial Perforation |
| LP | Lateral Perforation |
| SIMPLE | Semi-Implicit Method for Pressure-Linked Equations |
| RNG | Renormalization Group Analysis of Turbulence |
| k | Kinetic Energy |